Towards functional 3D-stacked electrospun composite scaffolds of PHBV, silk fibroin and nanohydroxyapatite: mechanical properties and surface osteogenic differentiation

Journal of Biomaterials Applications. 2016 Apr;30(9):1334-49.

Elena I. Paşcu[1], Paul A. Cahill[2], Joseph Stokes[1], Garrett B. McGuinness*[1]

1. Centre for Medical Engineering Research, School of Mechanical and Manufacturing Engineering, Dublin City University, Dublin, Ireland.

2. Vascular Biology and Therapeutics Laboratory, School of Biotechnology, Faculty of Science and Health, Dublin City University, Dublin 9, Ireland.

* Corresponding author: Centre for Medical Engineering Research, School of Mechanical and Manufacturing Engineering, Dublin City University, Ireland. Tel.: + 353 1 700 5423, e-mail: garrett.mcguinness@dcu.ie

Full Citation:

Paşcu EI, Cahill PA, Stokes J, McGuinness GB. Towards functional 3D-stacked electrospun composite scaffolds of PHBV, silk fibroin and nanohydroxyapatite: Mechanical properties and surface osteogenic differentiation. Journal of Biomaterials Applications. 2016 Apr;30(9):1334-49.

Copyright © 2016 (The Authors). **DOI: 10.1177/0885328215626047**

Abstract

Bone tissue engineering scaffolds have two challenging functional tasks to fulfil: to encourage cell proliferation, differentiation and matrix synthesis, and to provide suitable mechanical stability upon implantation. Composites of biopolymers and bioceramics combine the advantages of both types of materials, resulting in better processability, and enhanced mechanical and biological properties through matrix reinforcement. In the present study novel thick bone composite scaffolds were successfully fabricated using electrospun flat sheets of polyhydroxybutyrate - polyhydroxyvalerate (PHBV)/ nanohydroxyapatite (nHAp)/ silk fibroin essence (SF) (2% nHAp - 2% SF and 5% nHAp - 5% SF, respectively). Their potential as *in vitro* bone regeneration scaffolds was evaluated using mouse calvarian osteoblast cells (MC3T3-E1), in terms of morphology (SEM), cell attachment, cell proliferation, Col type I (COL I), osteopontin (OSPN), and bone alkaline phosphatase (ALP) activity (Quantitative Real Time Polymerase Chain Reaction [qRT-PCR], enzyme linked immunosorbent assay, immunocytochemistry). Electrospun polyhydroxybutyrate–polyhydroxyvalerate scaffolds were used as reference constructs. The results showed that the compressive and tensile mechanical properties of the scaffolds are dependent on the change in their composition, and the treatment these underwent. Furthermore, methanol-treated and autoclaved P2 (2% nanohydroxyapatite, 2% silk fibroin essence) samples appeared to exhibit more promising tensile properties. Additionally, the compressive tests results confirmed that the methanol pre-treatment and the autoclaving step lead to an increase in the P2 secant modulus when compared to the non-methanol treated ones, P2 and P5 (5% nanohydroxyapatite, 5% silk fibroin essence), respectively.

Both formulations of polyhydroxybutyrate–polyhydroxyvalerate/nanohydroxyapatite/silk fibroin essence composite promoted greater cell adhesion and proliferation than the

corresponding polyhydroxybutyrate–polyhydroxyvalerate control ones. Cells seeded on the composite fibrous scaffolds were extensively expanded and elongated on the fibre surface after 1 day in culture, whereas those seeded on the polyhydroxybutyrate–polyhydroxyvalerate scaffolds were not completely elongated. In addition, cells grown on P2 and P5 scaffolds had higher ALP activity when compared to those containing no nanohydroxyapatite/silk fibroin.

1. Introduction

Extracellular matrix (ECM) plays multiple roles within tissues, including bone [1]. It can be viewed as a dynamic network of molecules, secreted by the cells, that in turn regulates cell behaviour by modulating the proliferation and differentiation processes [2]. When mimicking the ECM, one should consider a variety of factors that influence the cellular functions and subsequent tissue maturation, such as the scaffold's architecture, physical characteristics, and biochemical properties [3, 4]. Further attention should be paid when choosing the materials and the fabrication techniques as the aim is to mimic the natural *in vivo* environment of the targeted cells in such a way as to recreate the missing host tissue.

There are a multitude of techniques used to replicate the ECM [5, 6], but electrospinning is probably the most intensively researched top-down method used to produce nonwoven nanofibrous scaffolds [7 - 9]. In this regard, recent studies have shown that nanofibrous structures developed using the electrospinning technology provide suitable conditions for the anchorage, migration, and differentiation of tissue cells, particularly bone cells [4,5,7].

A number of biodegradable biopolymers and composite solutions have been electrospun and analysed as hard tissue substitutes, such as polycaprolactone (PCL) [10], poly-lactic acid [11], hydroxyapatite - poly (DL-lactide) composite [12], silk, gelatine and chitosan [13 - 17].

Silk fibroin/silk fibroin essence (SF) has been shown to be a potent alternative for a multitude of biodegradable biopolymers, due to its mechanical properties, tunable architecture, and its demonstrated ability to support bone formation both *in vitro* and *in vivo* [18]. At the same time, silk is a thermally stable material, allowing processing over a wide range of temperatures (up to about 250 °C) without loss of functional integrity, which makes it a good candidate for autoclave systems [19].

Furthermore, there is particular interest in polyhydroxyalkanoates (PHA) as bio-derived and biodegradable polymers. One polymer in particular, poly(3-hydroxybutyrate-co-3-hydroxyvalerate) (PHBV), is known for its excellent biocompatibility and *in vivo* degradation products, specifically monomers that are normally present in the blood stream. In our recent study a composite solution made of PHBV, nHAp and SF was electrospun into novel thin fibrous sheets intended for bone tissue engineering [20]. The preliminary biological evaluation of these mats showed good cellular response as human bone-derived osteoblasts (hHOBs) proliferated after 3 days in culture and retained their morphology while presenting a flattened appearance and elongated shape on the surface of the fibres.

While nanofibre/microfibre scaffolds have been shown to favour the proliferation and alkaline phosphatase (ALP) production of osteoblast-like cell lines and bone marrow stromal cells, the materials used for the development of electrospun nanofibres are required to have properties specifically suitable for calcified hard tissues [21]. Ito *et.al* [21] used a biodegradable and biocompatible PHBV copolymer from a microbial polyester and electrospun it into a nanofibrous web that was covered with hydroxyapatite (HAp) as a result of immersion in simulated body fluid (SBF). The surface of the nanofibrous film showed enhanced cell adhesion over that of a cast film, while cell adhesion was not significantly

affected by the HAp/PHBV combination. Kim *et al.* [22] have electrospun SF and applied it as a biomaterial in bone and periodontal regenerative therapy due to its favourable biological properties. Results showed that the cell numbers and osteocalcin (OC) levels increased significantly with culture time. The human bone marrow stromal cells (BMSCs) exhibited a star-like shape and broad cytoplasmic extensions on the membrane. In the *in vivo* tests, a complete bony union across the defects was observed after 8 weeks, while complete bone formation with defect healing was detected at 12 weeks.

Other studies fabricated microporous, non-woven PCL scaffolds [23, 24]. After only one week, mesenchymal stem cells (MSCs) have infiltrated within the scaffold and abundant ECM formation was observed in the cell-polymer constructs. SEM results at four weeks demonstrated that the surfaces of the cell-polymer constructs were covered with multiple layers of cells. In addition, mineralization and COL I expression were observed.

Furthermore, Ngiam *et al.* [25] prepared poly-L-lactic acid (PLLA) and PLLA/collagen (50% PLLA+50% collagen; PLLA/Col) nanofibres using electrospinning. They mineralized these nanofibres using a modified alternating soaking method and assessed its biological properties using hHOBs. The results showed that the bone-like nanohydroxyapatite (nHAp) was successfully deposited on the PLLA and PLLA/Col nanofibres. They observed that the formation of nHAp on PLLA/Col nanofibres was faster and significantly more uniform when compared to the pure PLLA nanofibres. Based on these observations, the authors demonstrated that nHAp deposition on nanofibres is a promising strategy for early cell capture. Yunos *et al*. [26] designed bilayered constructs by combining electrospun poly-DL-Lactide (PDLLA) fibres and Bioglass®-derived scaffolds for development of osteochondral tissue replacement materials. Bioactivity studies in SBF showed that HAp mineralization decreased as the thickness of the PDLLA layer increased. A preliminary *in vitro* study using

chondrocyte cells (ATDC5) showed that cells attached, proliferated and migrated into the fibrous network, confirming the potential applicability of the bi-layered scaffolds in osteochondral defect regeneration. In contrast to these studies, in our previous study [20] we were able to incorporate the nHAp particles within the composite fibrous matrix by mixing the ceramic phase in the solution before electrospinning, thus avoiding the alternative SBF soaking step. The Energy Dispersive X-ray spectroscopy (EDX) results confirmed the presence of the nHAp particles inside and on the surface of the elecrospun fibres.

Cell adhesion behaviour and the proliferation rates on functional scaffolds are important parameters and determine the scaffolds quality and suitability for the targeted application [27]. The present biological study used mouse pre-osteoblast cells from bone-calvaria (MC3T3-E1) to evaluate the *in vitro* biocompatibility of the electrospun novel composite scaffolds in 3D form.

The present work used the same fibrous thin mats produced previously [20] to construct 3D electrospun scaffolds. While PHBV fibres formed the matrix structure of the scaffold, nHAp mimicked the ceramic part of the bone. Additionally, SF was hypothesized to enhance the mechanical and biological properties of the whole structure, important for osteointegration. The present study investigates the compressive mechanical properties of stacked scaffolds, and elaborates the effects of various phases of pre-treatment (methanol immersion, autoclaving) required to enhance the scaffolds' mechanical and biological properties. The acceptability of these properties must be considered with reference to the properties of comparable load bearing tissues. A more extensive biological characterisation is also presented over a longer timeframe (28 days compared to 3 days in the initial screening). The specific aim of this part of the study is to confirm osteoblastic phenotype expression of

MC3T3-E1 and confirm the expression levels of bone-related markers for one or more of these scaffolds to indicate whether they are suitable for further development.

2. Materials and methods

2.1. Materials

Nano-size (200 nm) hydroxyapatite was obtained from Sigma Aldrich, Ireland. Polyhydroxybutyrate-co-(3-hydroxyvalerate) with 2% valerate fraction (PHBV, M_W = 410,000 g/mol) was sourced from Good Fellow-UK. Chloroform was obtained from Lennox-UK. *Bombyx mori* silk fibroin essence (SF) was obtained from Huzhou Synergy, World Trade Co. Ltd, Republic of China. Methanol, Dulbecco's phosphate buffer solution (PBS), phalloidin- Fluorescein isothiocyanate (FITC), monoclonal anti-osteopontin were purchased from Sigma Aldrich, Ireland. Fetal Bovine Serum heat inactivated (FBS), Minimum Essential Media – Alpha (MEM)-alpha medium and antibiotic/ antimycotic were purchased from Bio-Sciences, Ireland. AlexiFluor 546 labelled Anti Mouse IgG antibody was purchased from Invitrogen, USA. Collagen I antibody-FITC was purchased from Biorbyt, UK; Alkaline phosphatase, Bone ELISA Kit from Antibodies, Germany and the primers (Mm_Spp1_1_SG QuantiTect Primer Assay (200) and Mm_Col1a1_1_SG QuantiTect Primer Assay (200)) from Qiangen, Ireland.

2.2 Methods

Samples preparation and testing

The samples to be tested were prepared as explained in our previous study [20]. Briefly, PHBV in powder form was dissolved in chloroform to which HAp nanoparticles had previously been added under sonication, followed by *Bombyx mori* SF addition. The present study tests samples of three different compositions (P0, P2 and P5 in Table 1) which were electrospun at either 15 kV and 2 ml/h (P0) or 10 kV and 5ml/h (P2, P5), as outlined in [20], and then subjected to one of three different post-treatment scenarios. In certain cases, dried

composite scaffolds were treated with methanol to make them insoluble by increasing β-sheet content (silk II) [28, 29]. These samples were immersed in pure methanol for 10 min, rinsed in distilled water several times and left to dry at room temperature for 24 h. Sample codes, indicating the composition are shown in Table 1. Furthermore, sample are coded as follows: (1) unmodified as-electrospun samples are called non-methanol and non-autoclaved samples (NAM), (2) samples used after methanol immersion are called methanol-treated (M) and (c) samples used after both methanol immersion and autoclaving are called methanol-treated and autoclaved (MA).

It should be noted that except for the FT-IR analysis and the tensile tests, where flat 2D sample were used, thick 3D samples prepared using the folding/ stacking technique outlined below were used for all compressive and biological tests. Furthermore, all samples were sterilised by means of autoclaving at 121°C for 20 min.

Tensile testing

For the tensile testing sets of six flat rectangular shaped samples were used. After the flat samples (40 mm × 10 mm) were manufactured, the tensile strength and the elastic modulus of the porous fibrous polymeric and composites samples were determined, using a Zwick/Roell Z500 N universal testing machine equipped with a 20 N load cell (Zwick GmbH, Ulm, Germany). The results were plotted with Test Xpert II (Zwick GmbH, Ulm, Germany). Samples were tested up to failure. The results were expressed in terms of average (+/- standard deviation) moduli and strengths [20].

Compressive testing

Sets of six electrospun fibrous rectangles were tested for each composite type using a Zwick/Roell Z500 N universal testing machine (Zwick GmbH, Ulm, Germany) equipped with a 5 kN load cell. Five electrospun flat membranes, each collected over a period of 20 min, were folded twice and squares of 1 cm x 1 cm were carefully cut, avoiding any raised edges. No pressure was applied before cutting the rectangular shapes (Figure 1). Constructs thickness varied from 0.3 mm for the P0 to 0.4 mm for P2 and P5 composites, respectively. The rectangles were compressed at a rate of 2 $mm \cdot min^{-1}$ until 80% strain was reached. Results are expressed in terms of the secant modulus for a stress of 0.4 MPa.

By means of comparison with other techniques, which either destroy the fibrous structure (laser welding, sintering) or may be time consuming (hydrospinning, which involves collecting fibres on top of a liquid reservoir and assembling them layer-by-layer to form a 3D scaffold), the stacking/ folding technique [30] can produce 3D constructs that retain their fibrous morphology and porosity (Figure 1).

Chemical analysis (FT-IR)

The chemical bonding structures present in the fibre were analysed using Fourier Transform Infrared Spectroscopy (Spectrum GX FT-IR) equipped with an ATR accessory Horizontal Attenuated Total Reflectance (HATR) with zinc selenide (ZnSe) crystal. To avoid scattering from large crystals a mixture of the sample to be tested (2 mg), which was previously cut into small pieces using a pair of scissors, and potassium bromide salt (200 mg) was ground in a marble mortar for 10 min. The ground mixture was then added into a die and pressed at 12 kPa for 15 min to form a translucent pellet, which allows the IR beam to pass through it [20].

Osteoblasts cells

MC3T3-E1 osteoblasts represent a suitable model for studying osteogenic development *in vitro*. They are the most commonly used cells in bone tissue engineering due to their capacity to differentiate into osteoblasts and to form calcified bone tissue *in vitro* [31].

Cell culture conditions

To determine cell attachment, MC3T3-E1 mouse calvarian osteoblast cells were cultured under standard tissue culture conditions (37 °C, 5% CO_2) in alpha-MEM medium (Gibco, USA) supplemented with 10% FBS and 1% antibiotic/antimycotic (Gibco, USA). All experiments were conducted with cells between passages 6-10. Each 3D scaffold was cut into circular discs (~ 15mm diameter), sterilized and placed in wells of a 24-well TCPS (Corning). The samples were sterilized by autoclaving in PBS at 121°C for 20 minutes. Prior to cell seeding, the cells were stored in culture medium in a CO_2 incubator for 1 hour, to promote protein absorbtion. The cells were trypsinized, the cell number was quantified and then the cells were seeded onto the samples, at a concentration of 30,000 cells/ml in 2 ml of medium (for SEM observation and cell proliferation) and 50,000 cells/ml in 2 ml of medium (for qRT-PCR, ELISA assay and the immunocytochemistry (ICC) techniques). The medium was changed every 3 days and the culture was stopped at day 1, 3, 5, 7, 14, 21 and 28. Construct P0-MA was used as the control scaffold, while P2-MA and P5-MA were the experimental constructs.

Cell number - DAPI staining

To assess cell attachment and number, samples were seeded with 30,000 cells/ml. At each time point the samples were stained with 4',6-diamidino-2-phenylindole (DAPI) (a DNA binding dye, to stain nuclei) and FITC-labelled Phalloidin (a fungal toxin with specific affinity for f-actin fibrils, to visualize cell cytoskeleton). Samples were fixed with 4%

formalin for 15 minutes and then rinsed with PBS. Afterwards, cells were permeabilized by treating them with 0.1% Triton X solution. After the removal of Triton X, samples were incubated in 5% PBS- Bovine Serum Albumin (BSA) solution for 1 hour at room temperature, to decrease non-specific absorption of the dyes. Afterwards, 1:200 dilution of FTIC-Phalloidin was applied to the samples for 40 minutes in the dark, followed by 1:1000 dilution of DAPI for 15 minutes in the dark.

Cell counting data were generated from counting the total number of cells (DAPI stained) in three separate fibrous constructs per time point, using Image J software. The cells were counted at the surface (in focus) of the scaffold. A minimum of five randomly selected visual fields per fibre construct were counted (at 10X magnification using a fluorescent microscope (Olympus, Japan)). The total number of DAPI stained cells was counted at four different time points (day 3, 7, 14 and 28 of culture and differentiation) and was presented as number of cells per day of co-culture.

Cell morphology

Cell morphology was assessed using Scanning Electron Microscope (SEM, EVO LS15 SEM/EDX from Zeiss, Germany). After removing them from the culture medium, the samples were washed with PBS and immersed in 2% glutaraldehyde for 30 minutes at 4°C, followed by serial dehydration in series of ethanol solution (50% - 10 minutes, 60% - 10 minutes, 70% - 30 minutes, 80 % - 10 minutes, 90% - 10 minutes, 95% - 10 minutes, 100% - 10 minutes, 100% - 10 minutes). The dehydrated samples were immersed in hexamethyldisilazane (HMDS) for 1 minute and dried at room temperature. Samples were coated with gold for 80 seconds using an *Edwards Pirani 501 Scancoat* sputtering coater and observed under the SEM.

Osteopontin (OSPN) and Collagen type I expression (COL I) - Immunnocytochemistry (ICC)

ICC is used to visualize the presence of a specific protein or an antigen in the cells. For ICC analysis, sample preparation involves fixing the target cells to a slide, in our case the three-dimensional thick scaffold. To ensure access of the antibody to its antigen, cells must be fixed and permeabilized. In an ideal situation, fixation would immobilize the antigens while retaining the native cellular architecture and permitting unhindered access of the antibodies to all the cells and subcellular compartments. To assess osteoblastic differentiation and ECM deposition, the expression of two of the three chosen bone markers (OSPN and COL I) was assessed for day 1, 3, 7, 14, 21 and 28. Furthermore, ELISA was used for alkaline phosphatase (ALP) levels quantification. Each marker was assessed on a different set of samples and P0-MA was used as the reference sample.

Osteopontin (OSPN)

For OSPN detection samples were stained with non-conjugated monoclonal anti-osteopontin (OPN46), a synthetic peptide, to bind osteopontin antigens. Samples were fixed with 4% formalin for 15 minutes and then rinsed with PBS. Afterwards cells were permeabilized by treating them with 0.1% Triton X- PBS for 10 minutes at room temperature. After removal of Triton X, cells were blocked with 5% BSA-PBS-1% Tween for 1 hour at room temperature or overnight at 4°C. Afterwards a 1:100 dilution of monoclonal anti-osteopontin was used for 1 hour followed by two washes with PBS-1% Tween for 5 minutes each, to wash away the non-specific binding. Afterwards, a 1:200 dilution of fluorescent secondary antibody containing 1% BSA was added for 1 hour in the dark, followed by a 1:1000 DAPI dilution for 15 minutes.

Collagen type I (COL I)

COL I expression was assessed using the same ICC protocol as for OSPN detection. A dilution of 1:100 COL I antibody conjugated to FITC-phalloidin (Biorbyt, a synthetic peptide to bind collagen type I antigens), followed by a 1:1000 DAPI dilution to bind the nuclei.

RNA Isolation and quantification of gene expression (qRT- PCR)

In order to quantify OSPN and COL I markers expression, pre-osteoblasts (MC3T3-E1) were seeded on three types of scaffold (P0-MA, P2-MA and P5-MA) and tissue culture plates (TCPS), at a density of 5 x 10^4 cells/cm^2. The total RNA was isolated following the protocol for the isolation of RNA using TRIsure (Bioline) at day 0 (prior to seeding), 1, 3, 7, 14, 21 and 28. The cells were lysed directly on the culture dish or scaffold by adding 1 ml of TRIsure per well and the cell lysate was pipetted several times to ensure sufficient cell disruption. Further, samples were incubated for 5 min at room temperature, followed by the addition of 0.2 ml of chloroform per 1 ml of TRIsure used, and capped tubes were shaken vigorously by hand for 15 seconds. Afterwards, samples were incubated for 2-3 min at room temperature and centrifugedat 12,000 g for 15 min at 2-8°C. During centrifugation samples would have separated into a pale green, phenol-chloroform phase, an interphase, and a colourless upper aqueous phase that contained RNA. The next step was RNA precipitation. This was done by transferring the aqueous phase to another tube without disturbing the interphase. Further, the RNA was precipitated by mixing it with cold isopropyl alcohol (0.5 ml of isopropyl alcohol per 1ml TRIsure), followed by incubation for 10 min at room temperature and centrifugation at 12,000 g for 10 min at 2-8°C. After removing the supernatant, the pellet was washed with 75% ethanol, adding at least 1 ml per TRIsure used.

The samples were vortexed and centrifuged at 7500 g and 2-8°C. After air-drying the pellet and dissolving it in Diethylpyrocarbonate (DEPC)-treated water, the samples were stored at -70°C before analysis. The isolated RNA was quantified by measuring the absorbance at 260 nm. Theoretically, an absorbance of 1 corresponds to 44 µg/ml of RNA. The 260/280 ratio of absorbance was used to assess the purity measurement using a Nanodrop spectrophotometer.

Finally, mRNA levels were measured by using qRT-PCR with the help of Rotor-Gene SYBR Green RT-PCR Kit for two bone phenotype markers (OSPN and COL I) and one house keeping gene (Glyceraldehyde 3-phosphate dehydrogenase [GADPH]). The reaction was carried out by using 12.5 µl of 2 X Rotor-Gene SYBR Green RT-PCR Master Mix with 10X and the necessary amount of water to complete the reaction mix to 50 µl. Then, the PCR reaction was carried out for 40 cycles with the following cycling conditions: initial denaturation (94 °C, 2 min), 40 cycles of denaturation (94 °C, 15 s), annealing (60 °C, 1 min), extension (72 °C, 1 min). Primer specificity was assessed beforehand. Final results are reported by $2^{-\Delta\Delta Ct}$ method.

Alkaline phosphatase (ALP) enzyme-linked immunosorbent assay (ELISA)

ALP is an enzyme expressed by cells and is an early marker of osteoblastic differentiation. ALP enzyme activity of the constructs was measured using an Alkaline Phosphatase Assay Kit from Antibodies (Germany) according to the supplier instructions. This ALP enzyme linked immunosorbent assay applies a technique called a quantitative sandwich immunoassay. The microtiter plate provided in the kit has been pre-coated with a monoclonal antibody specific for ALP. Standards or samples were then added to the microtiter plate wells and ALP, if present, bonded to the antibody pre-coated wells. In order to quantitatively determine the amount of ALP present in the sample, a standardized preparation of horseradish peroxidase (HRP)-conjugated polyclonal antibody, specific for

ALP, was added to each well to sandwich the ALP immobilized on the plate. The microtiter plate underwent incubation, and then the wells were thoroughly washed to remove all unbound components. Next, A and B substrate solutions were added to each well. The enzyme (HRP) and the substrate were allowed to react over a short incubation period. Only those wells that contain ALP and enzyme-conjugated antibody have exhibited a change in colour. The enzyme-substrate reaction was terminated by the addition of a sulphuric acid solution and the colour change was measured spectrophotometrically at a wavelength of 450 nm. Samples were run in triplicates and compared against the provided standards.

Statistical analysis

All results were expressed as means and standard deviations. Statistical significance of the differences among polymeric scaffolds (control) and composite samples was determined using the Student's t test. $*p < 0.05$ was considered statistically significant.

3. Results and discussions

3.1 Mechanical evaluation

For bone tissue engineering applications, the mechanical properties of the scaffold in both tension and compression are of direct interest. In our previous paper, only the tensile mechanical properties of non-methanol treated, non-autoclaved (NAM in the terminology of this paper) electrospun PHBV/ nHAp/SF thin fibrous scaffolds were investigated [20]. The present study explores the effects of methanol pre-treatment on its own, and then combined with autoclaving, on both the tensile and compressive properties of the 3D thick scaffolds. In order to induce a change in the protein configuration from the random coil conformation to the β –sheet conformation, thereby making it water insoluble [28, 29], the NAM samples

were immersed in pure methanol. Figure 2 presents the chemical spectra of these samples (FT-IR data), while Figure 3 shows the Young's modulus in tension for all NAM, M and MA samples. The results show a significant increase in the tensile modulus after methanol treatment for P2-M and P5-M relative to P0-M, suggesting that this led to conformation changes of SF from amorphous to β-sheet. Furthermore, P2-M samples exhibit a higher Young's modulus when compared to that of the P5-M. The FT-IR spectra of the composite before methanol treatment support these results (Figure 2A). Following the autoclaving pre-treatment the Young modulus of P2-MA and P5-MA is lower when compared to that of P0-MA, while that of P2-MA is higher in comparison with P5-MA. Additionally, the same increase in the tensile modulus can be observed when comparing the results for P2-M and P2-NAM. Interestingly, this trend was not evidenced when comparing P5-M to P5-NAM, suggesting that only certain concentrations of SF/nHAp that can be added to the polymer in order to improve the composite tensile properties.

The FT-IR spectrum of P2-NAM reveals SF characteristic amides: amide A at 3294 cm^{-1}, amide I between 1500-1600 cm^{-1}, amide II at 1380-1400 cm^{-1} and amide III at 1375 -1390 cm^{-1}, while the spectrum of the methanol treated samples reveals an increase in transmittance and shifted peaks for amide II and III suggesting that the β-sheet conformation change was induced for the samples treated with methanol [28].

In order to assess if the samples' chemical conformation and mechanical properties have changed after autoclaving, FT-IR and mechanical analyses were used to characterise the sterilised samples (MA). Figure 2B shows the FT-IR spectrum of the MA samples. It can be observed that the main signal was given by methanol, which indicated that a high amount of alcohol was present on the samples. This residue was so strong that it might have been masking the sample bands on the spectra. The methanol spectrum has been added in Figure

2C for comparison reasons. At this stage, a washing step using distilled water was included in order to remove the traces of methanol as described in the Methods section. The FT-IR results showed that the traces of methanol have been removed and that autoclaving did not affect the chemical conformation of the sample.

Figure 3 shows the tensile Young's modulus results for the NAM, M and MA samples. Figure 3 reveals that the tensile Young's modulus of P2-MA is lower than those of P2-M, while P5-MA slightly increases versus P5-M and the control P0-M. Furthermore, the Young's modulus of P2-MA samples were not significantly different to those of the P2-NAM samples, while P0-MA samples showed a significant increase in their Young's modulus after sterilisation compared to the P0-NAM and P0-M ones. From these tests, a clear difference emerges between the behaviours of the P0, P2 and P5 compositions with respect to the effect of the two treatments on tensile mechanical properties. Since autoclaving is expected to be part of the sterilisation process for such scaffolds, the MA sample properties are the most pertinent and the P2-MA sample appears to be the more promising of the two composite options in this respect. The P5 composition results in comparatively diminished tensile properties.

Figure 4 presents the secant modulus for the same group of samples. The compressive tests results showed that the methanol pre-treatment leads to an increase in the secant modulus of P2-M and P5-M samples when compared to P2-NAM and P5-NAM, respectively. Furthermore, autoclaving causes a decrease in the secant modulus of the P2-MA and P5-MA samples when compared to the P2-M and P5-M, respectively. Moreover, the secant modulus of the P2-MA sample is higher than of the corresponding NAM one, suggesting that the combination of methanol immersion and autoclaving treatments improved the secant modulus of the P2 composite sample. Unlike the results for the composite samples, P0-MA constructs

exhibited a decrease in the secant modulus when compared to the P0-NAM samples, results that suggest that the combination of treatments led to changes to the polymeric material in terms of its deformability under compressive loads. Furthermore, when comparing P2 versus P5, using samples that underwent the same pre-treatment, results show that P2 is again superior to P5 in terms of resistance to compressive loads. It was considered that autoclaving might act to promote formation of ordered beta sheets in the silk fibroin, a mechanism which would normally enhance overall mechanical integrity. However, the compressive and tensile results for M and MA composite samples showed no increase in this direction when compared to the NAM samples.

3.2 Biological evaluation of the electrospun three-dimensional scaffolds

Cell attachment and number - DAPI staining

Culture of MC3T3-E1 on electrospun fibrous scaffolds proved successful and osteogenic differentiation was observed. The MC3T3-E1 cells were able to attach and propagate on and within the fibrous structure (Figure 5). The counting of the DAPI stained cell nuclei indicated a statistically significant increase in the cell number for all types of electrospun composite constructs tested (P0-MA, P2-MA, P5-MA) from an average of 45 ± 4 cells per visual field (P0-MA), 74 ± 6 cells per visual field (P2-MA), 68 ± 6 cells per visual field (P5-MA) on day 1 to 183 ± 12 cells per visual field (P0-MA), 201 ± 12 cells per visual field (P2-MA), 84 ± 4 cells per visual field (P5-MA) on day 5 (Figure 6). The cell number decreased on day 3 and this could be attributed to cell proliferation in the depth of the scaffold as confirmed by the DAPI staining/confocal microscopy image of the fibrous structure at day 1 and 3 after seeding. On day 1, cell nuclei were visible in high number on the surface of the fibres, while on day 3 nuclei were also visible in the depth of the fibrous scaffold (Figure 5). Further, the number of cells remained fairly constant after day 5 and slightly decreased (Figure 6); day 7

(191 ± 14, p <0.05) and 28 (182 ± 9, p <0.05), indicating that the cells were differentiating (terminally differentiated/mature cells do not divide) rather than propagating at later time points in co-culture. When coupled with the cell number results, infiltration appears to be driven primarily by localized proliferation rather than coordinated cellular locomotion. The results are more promising when taking into account that there were no mechanical stimuli introduced to the *in vitro* cell culture (static cell culture) compared to the dynamic *in vivo* environment that would be found in the human body. The ICC results indicated that the MC3T3-E1 cultured on/in the fibre structure have stained positive for OSPN and COL I and showed increased bone marker expression starting with day 3 for OSPN and with day 7 for COL I, according to Figure 8 and Figure 9, respectively (32).

Figure 6 shows the total cell number. This increased dramatically from day 1 to day 5 in culture, and after that the cell number stabilized or slightly decreased indicating the generation of a more mature cell population that does not proliferate (divide).

Cell morphology - SEM

Figure 7 presents a selection of SEM micrographs showing the morphology and proliferation of MC3T3-E1 on the composite (P2-MA, P5-MA) and the polymeric (P0-MA) fibrous membranes after multiple days of culture. It can be seen that cells have attached to and proliferated on the surface of the membranes for the duration of the 28 days. Few osteoblast cells adhered to the composite and the polymeric scaffolds after 1 day of incubation on the P0-MA, P2-MA and P5-MA membranes. However, some cell spreading was observed after 3 days of incubation as the membranes were partially covered with MC3T3-E1 cells. As can be seen from the SEM images, the highest number of attached cells was detected on the P2-MA samples (P2-MA > P5-MA > P0-MA). The results are supported by the total cell number showed in Figure 6. Furthermore, after 3 days in culture P2-MA and

P5-MA membranes showed good cellular interaction and integration. On day 7 there was a pronounced difference between both the P2-MA and P5-MA membranes and the polymeric P0-MA membrane. More cells had attached to the composite test samples. They had spread well and the pseudopodia were stretched on these membranes as opposed to the cells seen on the polymeric control membrane. In addition, results revealed that the cells penetrated the pores. Furthermore, on both P2-MA and P5-MA membranes the cells had started to form sheets, indicating good attachment. On P0-MA scaffold, there were few cells attached and they were more widely separated. On day 14, approximately 90% of the surface area of the P2-MA membrane was covered with a thick layer of MC3T3-E1 cells. The SEM images demonstrate a confluent layer and full coverage of the surface at 14 days for the P2-MA composite and at day 21 for the P5-MA composite, while the P0-MA membrane exhibited partial coverage on day 28. Furthermore, ECM had formed on both test scaffolds by day 21. Results further demonstrate a slower rate of proliferation on the P0-MA polymeric membrane as compared to the P2-MA and P5-MA composite membranes. This may suggest that fibre composition might influence the cells proliferation rate as indicated by the cell number results, in particular for the P2-MA composite.

Osteopontin (OSPN) and Collagen type I (COL I) expression

Osteopontin (OSPN), known as bone sialoprotein I, is a highly phosphorylated sialoprotein that is a prominent component of the mineralized extracellular matrices of bone and teeth. The regulatory mecchanism of the osteopontin gene is incompletely understood. Different cell types may differ in the regulation of the OSPN gene. OSPN expression in bone occurs predominantly by osteoblasts and osteocyctes (bone-forming cells) as well as by osteoclasts (bone-resorbing cells) [33]. OSPN has been implicated as an important factor in bone remodelling playing a role in anchoring osteoclasts to the mineral matrix of bones.

Collagen type I alpha (COL I) is a human gene that encodes the major component of type I collagen, the fibrillar collagen found in most connective tissues. The COL I gene produces a component of type I collagen, called the pro-alpha1 (I) chain. Collagen is a protein that strengthens and supports many tissues in the body, including cartilage, bone, tendon and it is expressed during the initial period of proliferation and ECM biosynthesis [34].

In order to demonstrate bone formation by osteoblasts, the production of OSPN and COL I, two bone markers for osteoblasts, were evaluated [34 - 36]. OSPN and COL I expression was visualized by targeting the specific protein antigen in the cell via specific epitopes (red colour - OSPN, green colour - COL I). As presented in Figure 8, OSPN production increased in accordance with time up to day 28 for the MC3T3-E1 cells cultured on the P2-MA membranes. The same trend was apparent for the cells cultured on the P5-MA membranes, but not for cells cultured on the P0-MA membranes where OSPN expression increased gradually up to day 7 and decreased thereafter and this may be attributed to increased binding on the ECM deposited by cells [37]. OSPN levels were low at day 1, day 3, day 14, day 21 and day 28 for P0-MA membrane; at day 1, day 3, and day 7 for P2 and P5 membranes, which followed typical development for osteoblasts cultures [38]. In addition, based on the visual assessment of the confocal microscopy images, a difference in OSPN production between P0-MA and P2-MA, P5-MA membranes at day 21 and day 28 was observed. Furthermore, COL I expression was low at day 1, day 3 and day 7 for all the types of membranes followed by an increase in expression up to day 28 for P2-MA and P5-MA fibrous membranes (Figure 9). Control staining of non-seeded composite fibrous scaffold was performed in order to exclude primary, secondary antibody and DAPI staining binding on the fibres. Furthermore, representative merged and split images of OPN and DAPI, respectively COL I and DAPI are presented.

Quantitative real time-PCR

To further evaluate osteogenic differentiation on the scaffold surfaces, qRT-PCR measurements of osteogenic markers were performed. The expression of OSPN and COL I was determined using primers and probes specific for each osteogenic marker gene and was normalised to the housekeeping gene GAPDH. Gene expression levels were expressed as fold changes relative to the expression of the control sample (cells seeded on TCPS). Figure 11 presents the results as (a) comparison between control, P0 and P5 and (b) P2 fibrous membranes. At day 14, 21, and 28 MC3T3-E1 cells cultured on the P0 and P2 scaffolds expressed significantly higher mRNA levels for the OSPN gene ($p < 0.05$) when compared to the cells cultured on the TCPS plate and P5 scaffolds (Figure 10a). OSPN expression by MC3T3-E1 cells grown on the P0 scaffold increased more than 50 fold on day 14 and more than 200 fold on 21 day. MC3T3-E1 cells cultured on the P2 composite membranes evidenced an increase in OSPN gene expression (Figure 10b). Further, higher mRNA levels for COL I gene ($p < 0.05$) were observed for MC3T3-E1 cells cultured on P0 (Figure 11a) and P2 scaffolds (Figure 11b) as compared to P5 levels for day 21 and day 28. Moreover, COL I expression increased 120 fold on day 21 and 28 on P15 fibrous membrane and almost 35 fold on P2 composite membrane when compared to gene expression for cells cultured on TCPS plate. It should be noted that the medium used for these studies was not supplemented with ascorbic acid, which has been shown to initiate the formation of a collagenous ECM and synthesis of several osteoblast-related proteins [38 - 40].

Bone alkaline phosphatase (ALP) activity (ELISA assay)

Differentiation on the various substrates was characterised using bone alkaline phosphatase (ALP) as an early bone differentiation marker. Bone ALP, an ectoenzyme produced by osteoblasts, is believed to be involved in the degradation of inorganic

pyrophosphate, while providing sufficient local concentration of phosphate or inorganic pyrophosphate for the mineralization process to continue after its initiation [40]. Among the various biological functions of the osteoblasts, the secretion of alkaline phosphatase (ALP) is an important indicator determining the activity of the cells on a scaffold [41]. Cells adhering to P2 scaffolds exhibited significantly higher activity of the enzyme than on the P5 and the P0 scaffolds on day 21 and day 28, while P5 scaffolds exhibited higher activity levels on days 1, 3, 5 and 14 (Figure 12). ALP kinetics show a significant increase in the specific activity of the enzyme on P0 and P5 porous scaffolds at day 1 and day 3, followed by a decrease at day 5 and day 7. In contrast, the pattern of ALP activity on P2 samples does not resemble the other two constructs, which consists of a slow increase over the first week (days 1, 3, 5, 7), with an increase for days 14, 21 and 28. We observed two peaks in the activity of cells cultured on P5 at day 3 and day 14, while cells cultured on P2 scaffolds exhibited one peak in activity at day 28.

Conclusions

The mechanical results showed that the tensile Young's modulus of the composite fibres decrease when the content of the nHAp and SF phase is increased from 2% to 5%. This can perhaps be attributed to the lack of sufficient interfacial interaction between the nHAp and SF phases, respectively and the polymeric matrix. In terms of the compressive strength the composites samples properties were comparable to some load-bearing tissues as shown by Kurkijarvi *et al.* [42]. Additionally, it was considered that the inclusion of SF could reduce the solubility of composite samples in the cell culture medium and improve the mechanical properties by changing the configuration of the protein, from random coil conformation to β – sheet, after immersion in methanol [43, 44]. The results proved there was a significant

increase in the tensile strength for the composite sample of P2 and P5 after methanol treatment, consistent with the expected conformation changes to the silk fibroin.

In terms of the *in vitro* biological assessment, it can be concluded that all the scaffolds supported cellular attachment, as indicated by the cell count number and DAPI staining. Both analyses give an indication of a significant increase in cell number (and therefore as a result, cell proliferation) since the number of cells (dead or alive) within the scaffolds/mm^3 is greater than the number seeded initially. Furthermore, over the 28 day period, cell number for each group of scaffolds increased significantly indicating cellular proliferation. In the first five days more cells attached to the composite scaffolds (P2-MA and P5-MA) when compared to P0-MA samples. Additionally, there were significant differences between the number of cells attached on the P2-MA samples when compared to those observed on the P5-MA samples at day 7, 14, 21 and 28, respectively. Furthermore, extensive ECM formation and cell growth were observed after 14 days.

Enhanced osteoblast proliferation and differentiation was clearly evident by the increased levels of ALP, COL I and OSPN mRNA expression in cells cultured on the P2-MA composite fibrous construct as opposed to the P0-MA polymeric fibrous structure. These results also evidence that the cells are healthy and alive since they differentially express COL I, OSPN and ALP activity over time. Particular interest was paid to whether or not these fibrous scaffolds could support the osteoblastic phenotype expression of MC3T3-E1 and analyses of the expression levels of bone-related markers (OPN, COL I and ALP) were conducted in this direction. In this context, cells adhering to the P2-MA scaffolds exhibited significantly higher activity of ALP when compared to cells grown on P5-MA and the P0-MA at day 21 and day 28, respectively. These data cannot be attributed to a higher number of adherent cells and enhanced proliferation on P2-MA as compared to P0-MA and P5-MA at

the indicated time points. On the contrary, the ALP activity of the cells grown on P0-MA was the lowest at any given time point, despite the relatively high number of cells attached on its surface.

MC3T3-E1 cultured on the surface of P2-MA composite exhibited the greatest amount of OPN gene expression at all given time points when compared to cells cultured on the P0-MA and P5-MA constructs. This resulted in the greatest extent of mineralization for the cells grown on the surface of P2-MA, followed by that for the cells grown on P5 and P0, respectively. Compared to the P0-MA scaffolds, the composite materials supported osteoblast maturation, increasing the secretion of bone matrix, which aids in bone regeneration. The findings of this work support the hypothesis that the proposed composite scaffolds enhance the osteoblast phenotype and suggest that P2-MA and P5-MA scaffolds are appropriate cell carriers for osseous tissue engineering when compared to the PHBV polymer scaffolds (P0-MA). Taking the results as a whole, the P2-MA composition exhibits more promising properties than the P0-MA or P5-MA compositions, most notably with respect to the secant modulus values and OSPN and Col I expression.

The relevance of these results is not only in the fact that the structures obtained were comparable to the natural extracellular matrix, mimicking its morphology, but also that their physico-chemical and biological properties allow their use as potential bone - cells supports.

Declaration of Conflicting Interests

The author(s) declared no potential conflicts of interest with respect to the research, authorship and/or publication of this article.

Funding

The author(s) disclosed receipt of the following financial support for the research, authorship, and/or publication of this article: This research has been supported by an IRCSET (Irish Research Council for Science and Technology) EMBARK Initiative Scholarship.

References

1. Eap S, Ferrand A, Palomares CM, Hébraud A, Stoltz JF, Mainard D, Schlatter G, Benkirane-Jessel N, *Electrospun nanofibrous 3D scaffold for bone tissue engineering*, Biomed. Mater. Eng. 2012, 22 : 137-141.

2. Gentili C, Cancedda R, *Cartilage and bone extracellular matrix*, Curr. Pharm. Des. 2009, 15: 1334-1348.

3. Chan BP and Leong K W, *Scaffolding in tissue engineering: general approaches and tissue-specific considerations*, Eur. Spine J. 2008, 17: 467–479.

4. Annabi N, Vrana NE, Zorlutuna P, Dehghani F and Khademhosseini A, Engineering Biomimetic Scaffolds. In : Motta A and Migliaresi C (eds), *Scaffolds for Tissue Engineering: Biological Design, Materials, and Fabrication*, Pan Stanford Publishing Pte. Ltd Stanford , 2014, pp. 400.

5. Liu H, Ding X, Zhou G, Li P, Wei X and Fan Y, *Electrospinning of Nanofibers for Tissue Engineering Applications*, J. Nanomat. 2013 , 495708.

6. Luo CJ, Stoyanov SD, Stride E, Pelan E, Edirisinghe M, *Electrospinning versus fibre production methods: from specifics to technological convergence*, Chem. Soc. Rev. 2012, 13: 4708-4735.

7. Kanani AG, Bahrami SH, *Review on Electrospun Nanofibers Scaffold and Biomedical Applications*, Trends Biomater. Artif. Organs 2010, 24: 93-115.

8. Zhang Y, Venugopal J R, El-Turki A, Ramakrishna S, Su B, and Lim C T, *Electrospun biomimetic nanocomposites for bone tissue engineering*. Biomater. 2008, 29: 4314–4322.

9. Mikos AG and Kretlow J D, *Review: mineralization of synthetic polymer scaffolds for bone tissue engineering*, Tissue eng. 2007, 13: 927–938.

10. Patrício T, Glória A, Bartolo P*, Mechanical and Biological Behaviour of PCL and PCL/PLA Scaffolds for Tissue Engineering Applications*, Chem. Eng. Trans. 2013, 32: 1645–1650.

11. Kim H-W, Lee H-H, and Knowles JC, *Electrospinning biomedical nanocomposite fibers of hydroxyapatite/poly(lactic) acid for bone regeneration*, J. Biomed. Mat. Res. Part A 2006, 79: 643–649.

12. Cui W, Li X, Zhou S, and Weng J*, In situ growth of hydroxyapatite within electrospun poly(DL-lactide) fibers*, J.Biomed. Res. Part A, 82 (2007) 831–841.

13. Li C, Vepari C, Jin H-J, Kim H J, and Kaplan D L, *Electrospun silk-BMP-2 scaffolds for bone tissue engineering,* Biomater. 2006, 27: 3115–3124.

14. Cui W, Li X, Chen J, Zhou S, and Weng J, *In situ growth kinetics of hydroxyapatite on electrospun poly(DL-lactide) fibers with gelatin grafted*, Cryst. Growth Des. 2008, 8: 4576–4582.

15. Xue J, Feng B, Zheng R , Lu Y, Zhou G, Liu W, Cao Y, Zhang Y, Zhang WJ, *Engineering ear-shaped cartilage using electrospun fibrous membranes of gelatin/polycaprolactone*, Biomater. 2013, 34: 2624-2631.

16. Correia C, Bhumiratana S, Yan LP, Oliveira AL, Gimble JM, Rockwood D, Kaplan D L, Sousa RA, Reis RL., Vunjak-Novakovic G, *Development of silk-based scaffolds for tissue engineering of bone from human adipose-derived stem cells*, Acta Biomater. 2012, 8: 2483-2492.

17. Nwe N, Furuike T, Tamura H, *The Mechanical and Biological Properties of Chitosan Scaffolds for Tissue Regeneration Templates Are Significantly Enhanced by Chitosan from Gongronella butleri*, Mater. 2009, 2: 374-398.

18. Vepari C. and. Kaplan D.L*., Silk as a biomaterial*, Prog. Polym. Sci. 2007; 32: 991-1007.

19. Zhang X, Reagan MR and Kaplan DL, *Electrospun silk biomaterial scaffolds for regenerative medicine*, Adv. Drug Deliv. 2009, 61: 988-1006.

20. Paşcu E. I., Stokes J.,. McGuinness G. B,*Electrospun composites of PHBV, silk fibroin and nano-hydroxyapatite for bone tissue engineering*, Mater. Sci Eng. C. 2013, 33: 4905–4916.

21. Ito Y, Hasuda H, Kamitakahara M, Ohtsuki C, Tanihara M, Kang IK, and Kwon O.H., *A Composite of Hydroxyapatite with Electrospun Biodegradable Nanofibers as a Tissue Engineering Material*, J Biosci. Bioeng. 2005, 100: 43-49.

22. Kim KH, Jeong L, Park HN, Shin SY, Park WH, Lee SC, Kim TI, Park YJ, Seol YJ, Lee YM, Ku Y, Rhyu IC, Han SB, and Chung CP, *Biological efficacy of silk fibroin nanofiber membranes for guided bone regeneration*, J Biotechnol. 2005, 21: 327-339.

23. Shin SH, Purevdorj O, Castano O, Planell J. and Kim HW, *A short review: Recent advances in electrospinning for bone tissue regeneration*, J Tissue Eng. , 2012, 3 : 2041731412443530

24. Li W-J, Danielson K G, Alexander P G, and Tuan R S, *Biological response of chondrocytes cultured in three-dimensional nanofibrous poly(ε-caprolactone) scaffolds*, J. Biomed. Research 2003, 67:1105–1114

25. Ngiam M, Liao S, Patil AJ, Cheng Z, Yang F, Gubler MJ, Ramakrishna S, and Chan CK, *Fabrication of Mineralized Polymeric Nanofibrous Composites for Bone Graft Materials*, Tissue Eng. Part A 2009, 15: 535-546.

26. Yunos DM, Ahmad Z, Salih V, Boccaccini AR*, Stratified scaffolds for osteochondral tissue engineering applications: electrospun PDLLA nanofibre coated Bioglass®-derived foams*, J. Biomater. Appl. 2013, 5: 537-551.

27. Wutticharoenmongkol P, Pavasant P, and Supaphol P, *Osteoblastic Phenotype Expression of MC3T3-E1 Cultured on Electrospun Polycaprolactone Fiber Mats Filled with Hydroxyapatite Nanoparticles*, Biomacromolecules 2007, 8: 2602-2610.

28. Hardy JG, and Scheibel TR,*Composite materials based on silk proteins*, Prog. Polym. Sci. 2010, 35: 1093-1115.

29. Mobini S, Solati-Hashjin M, Peirovi H, Samadikuchaksaraei A, *Synthesis and characterization of fiber reinforced polymer scaffolds based on natural*

fibers and polymer for bone tissue engineering application, Iran. J. Biotech., 2012, 10:184-190.

30. Madurantakam P A, Rodriguez I A, Garg K, McCool J M, Moon PC, and Bowlin G. L., *Compression of Multilayered Composite Electrospun Scaffolds: A Novel Strategy to Rapidly Enhance Mechanical Properties and Three Dimensionality of Bone Scaffolds*, Adv. Mater. Sci. and Eng., 2013, Article ID 561273, 9 pages doi:10.1155/2013/561273

31. Beck Jr. GR, Zerler B, and Moran E, Phosphate is a specific signal for induction of osteopontin gene expression, PNAS; Proc. Natl. Acad. Sci, 2000, 97 : 8352-8357

32. Idris S.B., Arvidson K., Plikk P., Ibrahim S., Finne-Wistrand A., Albertsson A.C., Bolstad A.I., and Mustafa K., *Polyester copolymer scaffolds enhance expression of bone markers in osteoblast-like cells*., J. Biomed. Mater. Res .A, 2010, 94: 631-634.

33. Jaquiéry C., Schaeren S., Farhadi J., Mainil-Varlet P., Kunz C., Zeilhofer H.F. , Heberer M., Martin I., In vitro Osteogenic Differentiation and In vivo Bone-Forming Capacity of Human Isogenic Jaw Periosteal Cells and Bone Marrow Stromal Cells, Ann. Surg. 2005, 242: 859-867.

34. Lin Z, Solomon KL, Zhang X, Pavlos NJ, Abel T, Willers C, Dai K., Xu J, Zheng Q, and Zheng M, *In vitro Evaluation of Natural Marine Sponge Collagen as a Scaffold for Bone Tissue Engineering*, Int. J. Biol. Sci. 2011, 7: 968-977.

35. Marom R, Shur ., Solomon R, Benayahu D, *Characterization of adhesion and differentiation markers of osteogenic marrow stromal cells*., J. Cell. Physi. 2005, 202: 41-48.

36. Stein GS, Lian JB, Montecino M, van Wijnen AJ, Stein JL, Javed A, and Zaidi K., Involvement of nuclear architecture in regulating gene expression in bone cells, In: L G R PB Bilezikian, GA Rodan (eds) *Principles of Bone Biology*, Florida : Academic Press, 2002, pp. 169-188.

37. Rodriguez-Lorenzo LM, Saldaña L, Benito-Garzón L, García-Carrodeguas R, de Aza S, Vilaboa N, Román JS, *Feasibility of ceramic-polymer composite cryogels as scaffolds for bone tissue engineering*, J Tissue Eng Regen Med. 2012, 6: 421-433.

38. Franceschi RT, Iyer BS, Cui Y, *Effects of ascorbic acid on collagen matrix formation and osteoblast differentiation in murine MC3T3-E1 cells*, J Bone Miner Res. 2004, 9: 843-854

39. Xiao G, Cui Y , Ducy P, Karsenty G, and Franceschi RT, *Ascorbic Acid-Dependent Activation of the Osteocalcin Promoter in MC3T3-E1 Preosteoblasts: Requirement for Collagen Matrix Synthesis and the Presence of an Intact OSE sequence*, Mol Endocrinol. 1997, 11: 1103-1113.

40. Dhandayuthapani B, Yoshida Y, Maekawa T, and Kumar D S, *Polymeric Scaffolds in Tissue Engineering Application: A Review*, Int. J Polymer Sci. 2011; 1-19. Article ID 290602.

41. Sombatmankhong K, Sanchavanakit N, Pavasant P, and Supaphol P*, Bone scaffolds from electrospun fiber mats of poly(3-hydroxybutyrate),poly(3-*

hydroxybutyrate-co-3-hydroxyvalerate) and their blend, Polymer 2007, 48: 1419-1427

42. Kurkijarvi JE, Nissi MJ, Kiviranta I, et al. Delayed gadolinium-enhanced MRI of cartilage (dGEMRIC) and T–2 characteristics of human knee articular cartilage: Topographical variation and relationships to mechanical properties. Magn. Reson. Med 52 (2004) 41–46.

43. Hardy JG and Scheibel TR, *Composite materials based on silk proteins*, Progress in Polymer Science *2010 35:* 1093-1115.

44. Mobini S, Solati-Hashjin M, Peirovi H, Samadikuchaksaraei A, *Synthesis and characterization of fibre reinforced polymer scaffolds based on natural fibres and polymer for bone tissue engineering application,* Iranian Journal of Biotech 2012, 10: 184-190.

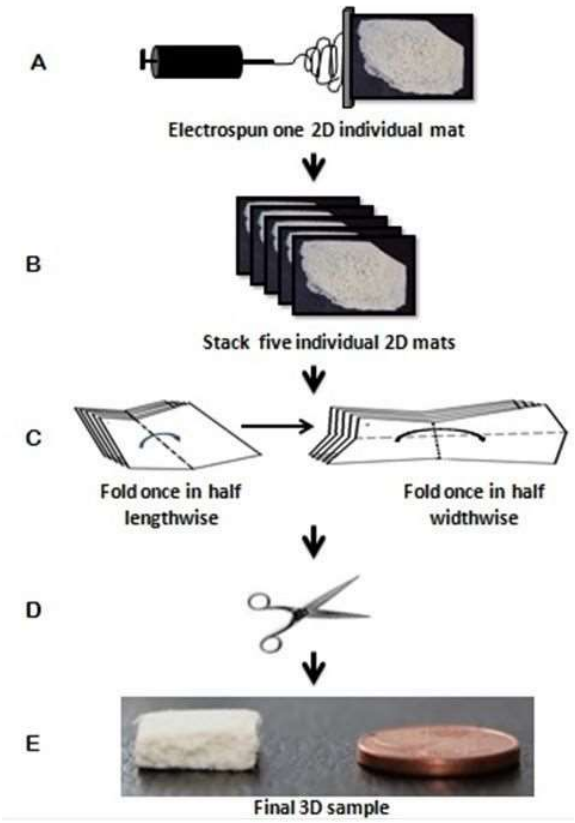

Figure 1. Diagram of the 3D fibrous construct which is manufactured as follows: (a) Electrospinning one individual two-dimensional mat (5 cm x 5 cm) (b) Stacking five such individual mats. (c) Manually folding the stacked electrospun mats twice. (d) Cutting the edges of the folded stacked group of mats using a scissors. (e) The final construct was composed of several stacked fibrous sheets.

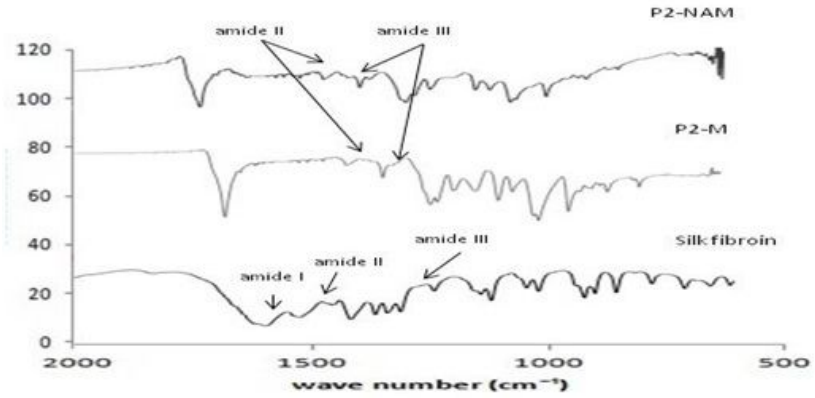
P2-NAM
amide II
amide III
P2-M
amide III
Silkfibroin
amide II
amide I
120
100
80
60
40
20
0
2000
1500
1000
500
wave number (cm⁻¹)

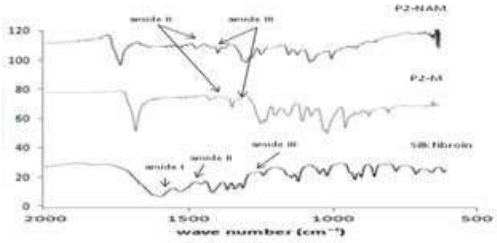
P2-NAM
P2-M
Silkfibroin
wave number (cm⁻¹)

A

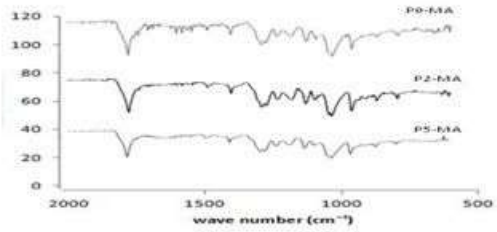
P0-MA
P2-MA
P5-MA
wave number (cm⁻¹)

B

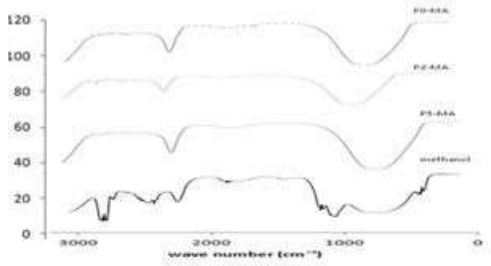
P0-MA
P2-MA
P5-MA
methanol
wave number (cm⁻¹)

C

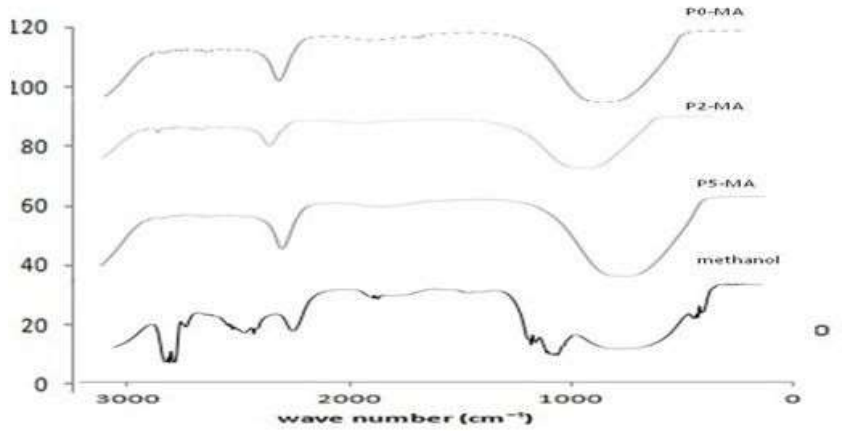

Figure 2. a) FT-IR spectra of P2 composite before and after immersion in pure methanol for 10 min at room temperature, b) FT-IR spectra of methanol treated-autoclaved samples (MA) after the washing step

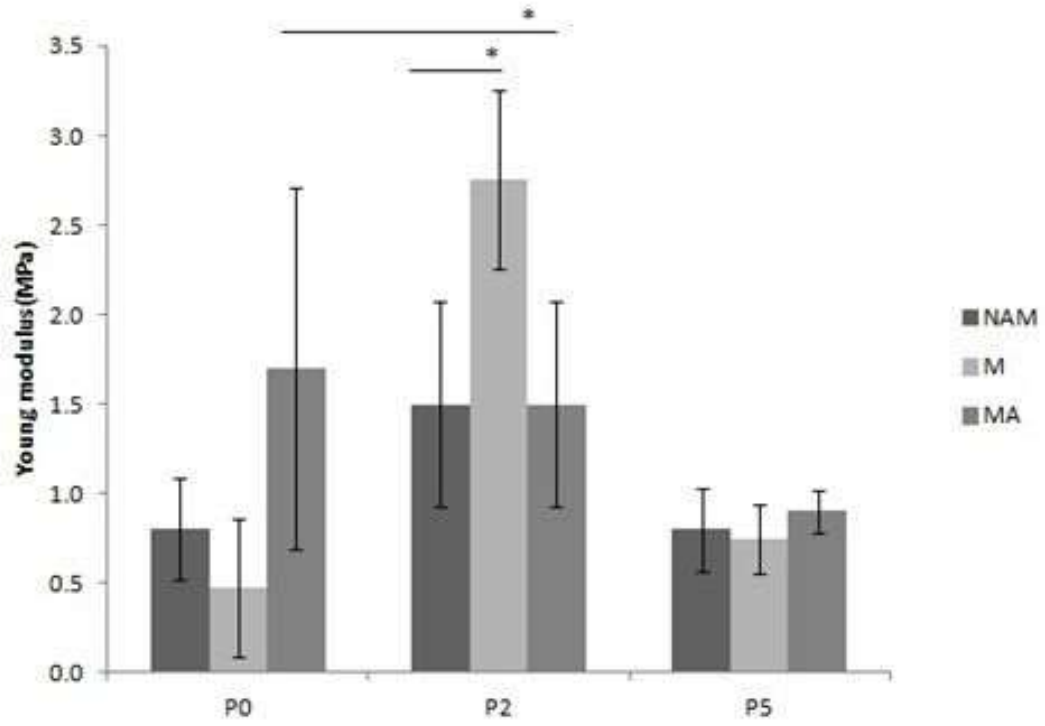

Figure 3 Young's modulus in tension of all pre-treated and non-treated P0, P2 and P5 samples (n = 6, p <0.05)

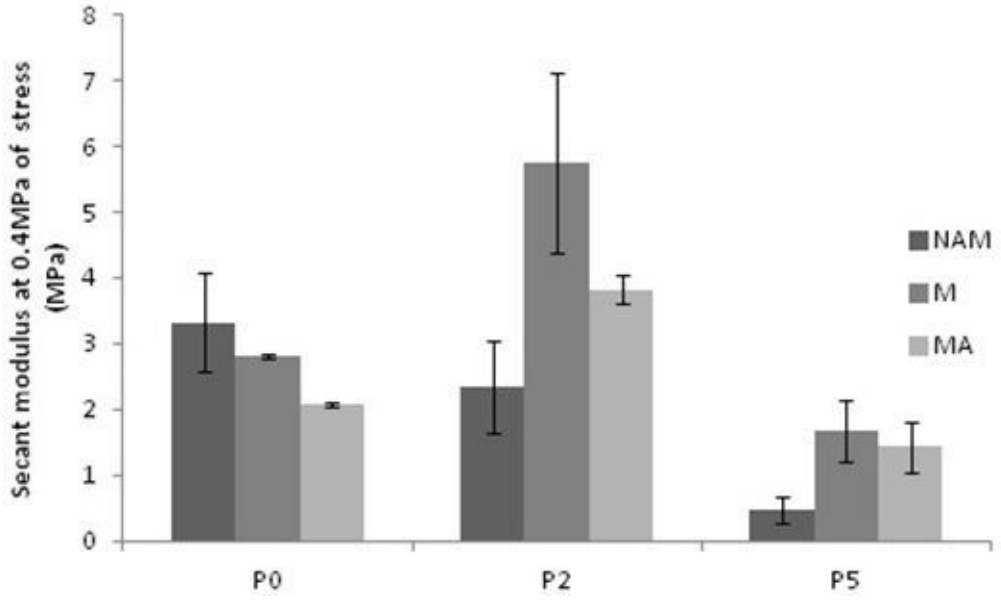

Figure 4. Compressive secant modulus of all pre-treated and non-treated P0, P2 and P5 samples (n = 6, p <0.05)

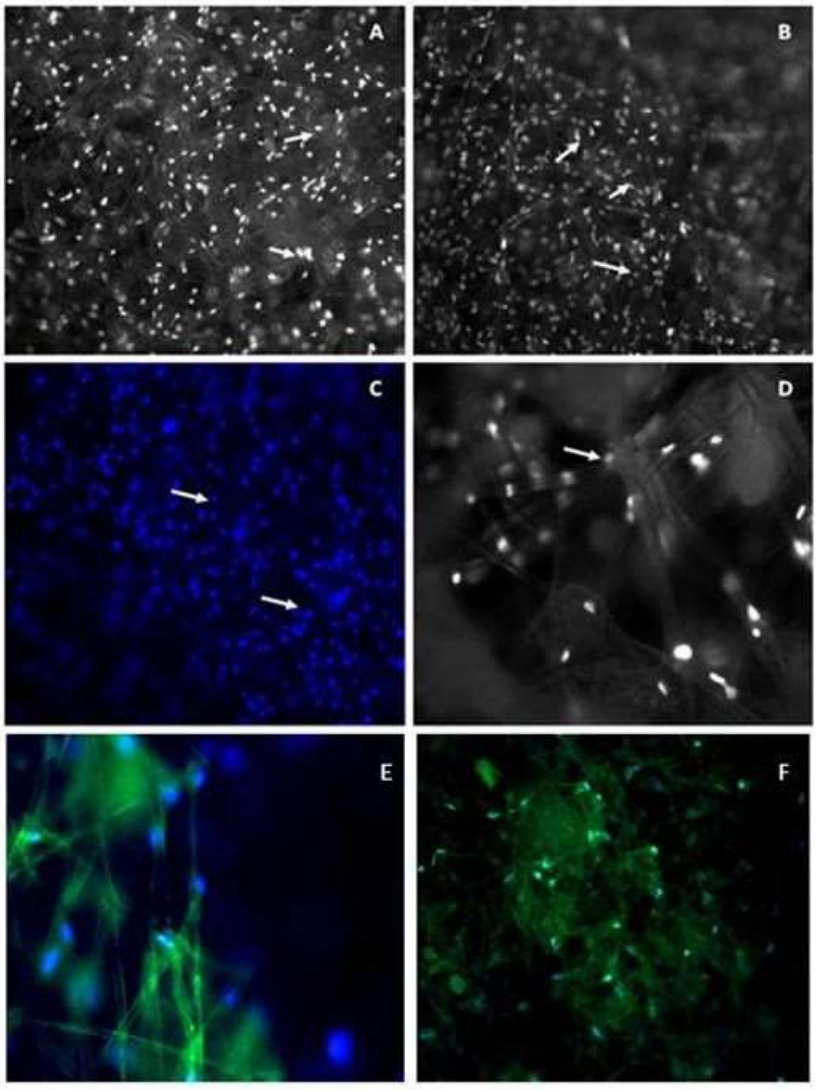

Figure 5. DAPI staining/confocal microscope image of P2--MA at (A) day 1 (B-D) day 3 after seeding, with arrows showing cells (A) attached on the outer fibrous layer of the scaffold and (B-D) cells infiltrated within the fibrous structure. (A-C) 10X magnification (D) 20X magnification

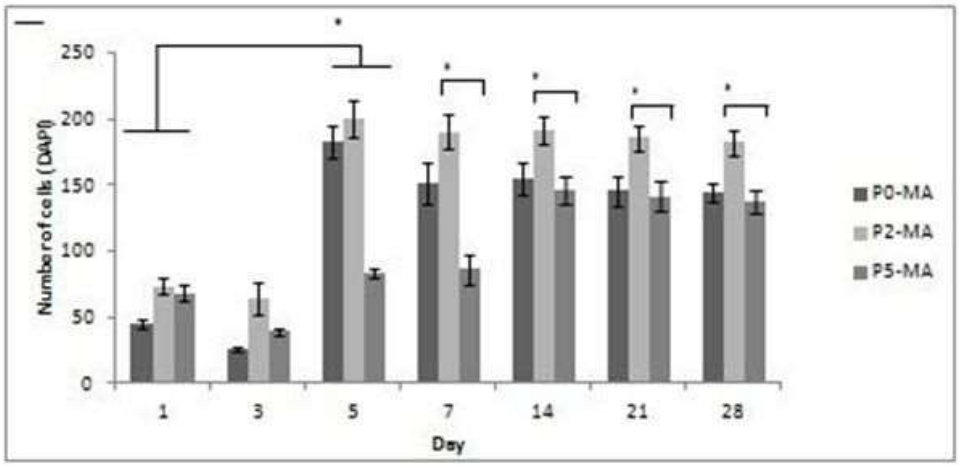

Figure 6. Total cell number per visual field (10X magnification) (n = 5, $p < 0.05$)

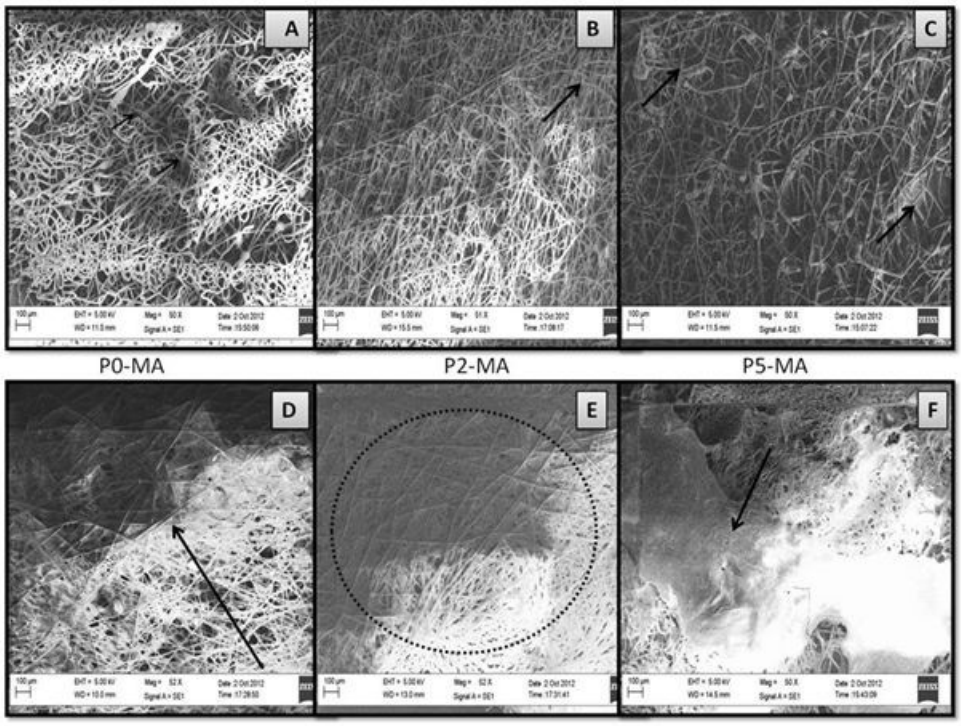

Figure 7. SEM micrographs of MC3T3-E1 cells grown on composite and polymeric fibrous membranes after 1 (A-C) and 28 (C-E) days in culture. Cell seeding density was 5 x 10^4 cells/ml.

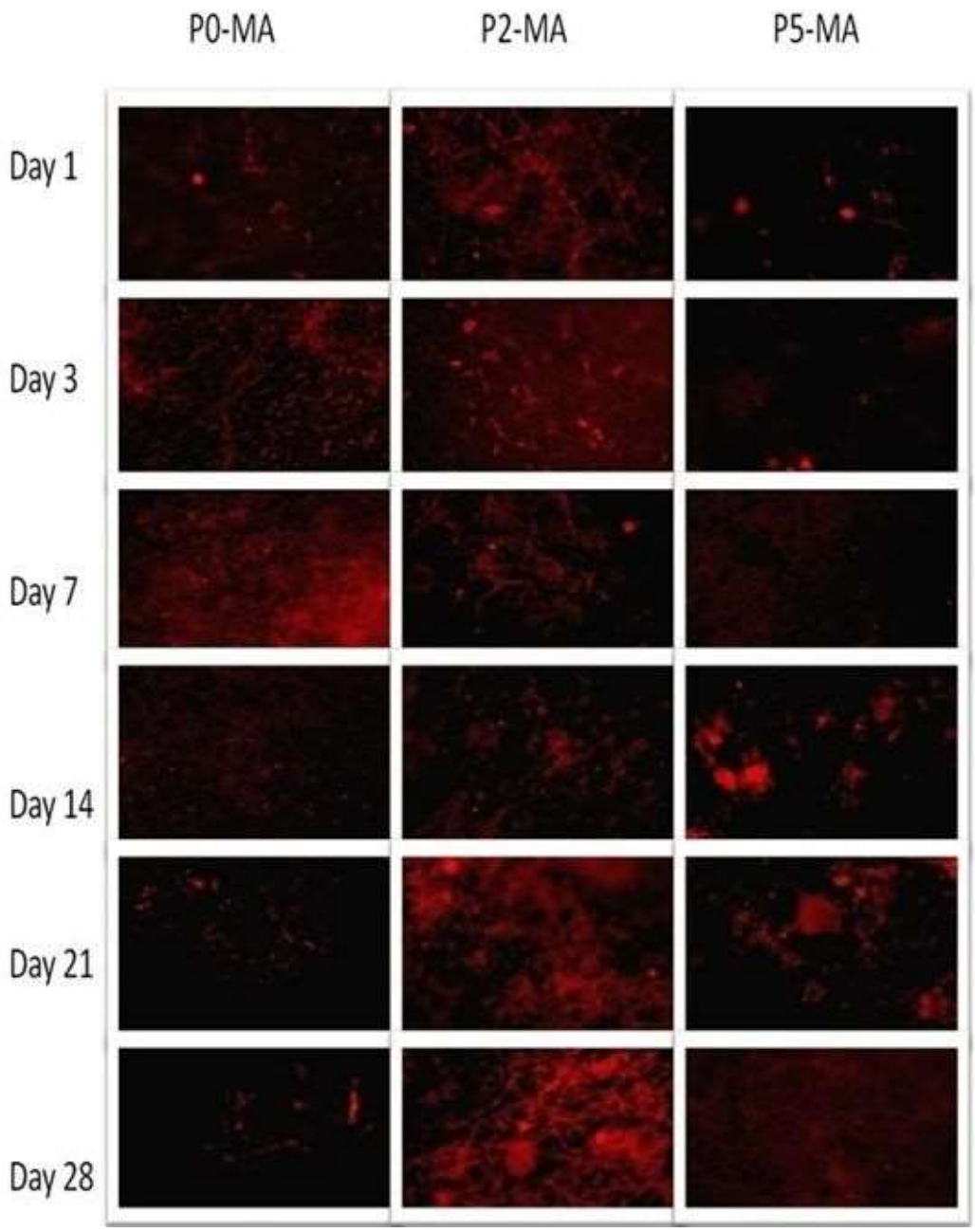

Figure 8. Osteopontin expression on P0_-MA, P2-MA and P5-MA fibrous polymeric and composite membranes after 1, 3, 7, 14, 21 and 28 days in culture. Cell seeding density was 5 x 10^4 cells/ml. Magnification 4X

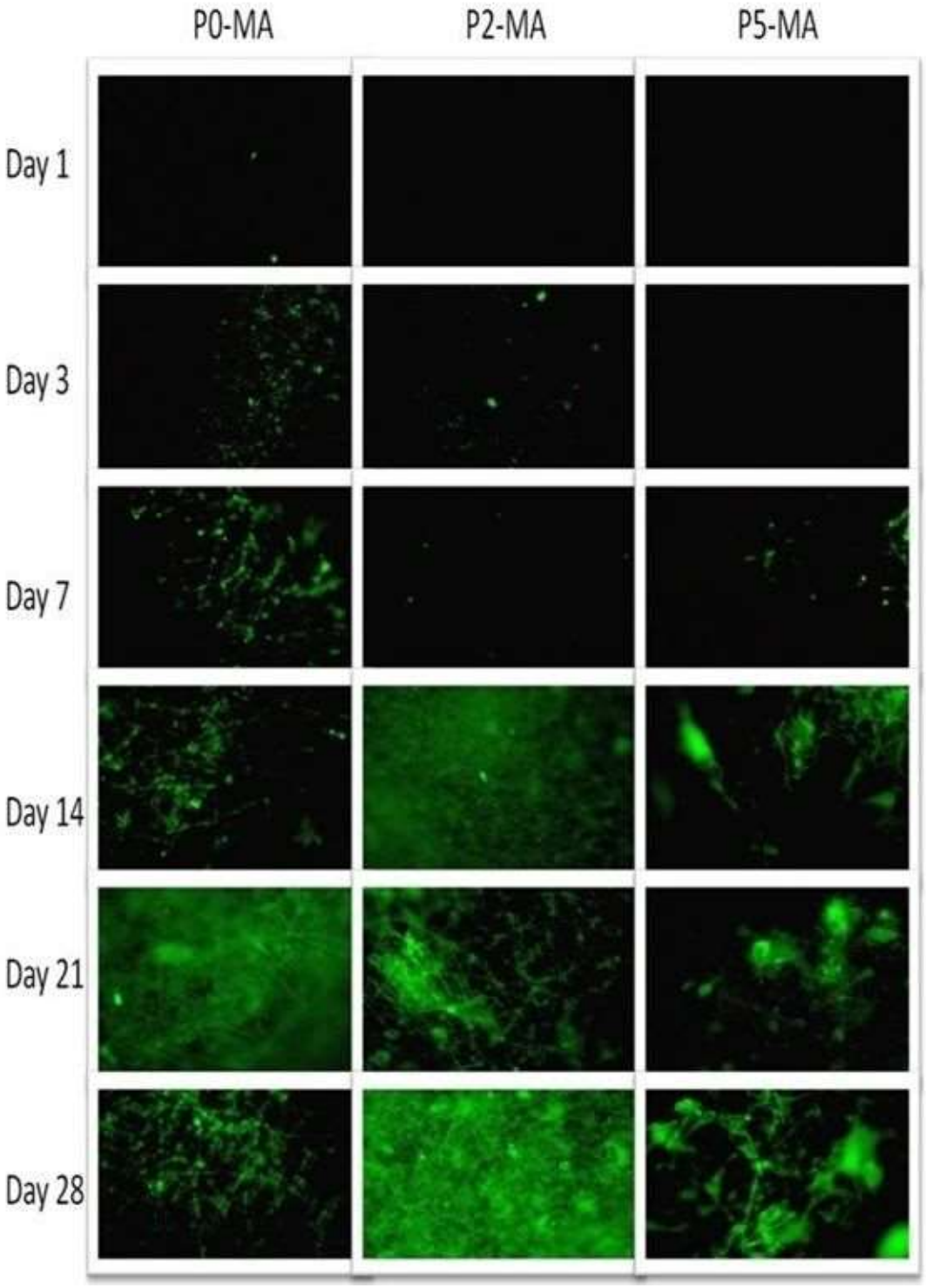

Figure 9. Collagen type I expression on P0--MA, P2-MA and P5-MA fibrous polymeric and composite membranes after 1, 3, 7, 14, 21 and 28 days in culture. Cell seeding density was 5 x 10^4 cells/ml. Magnification 4X

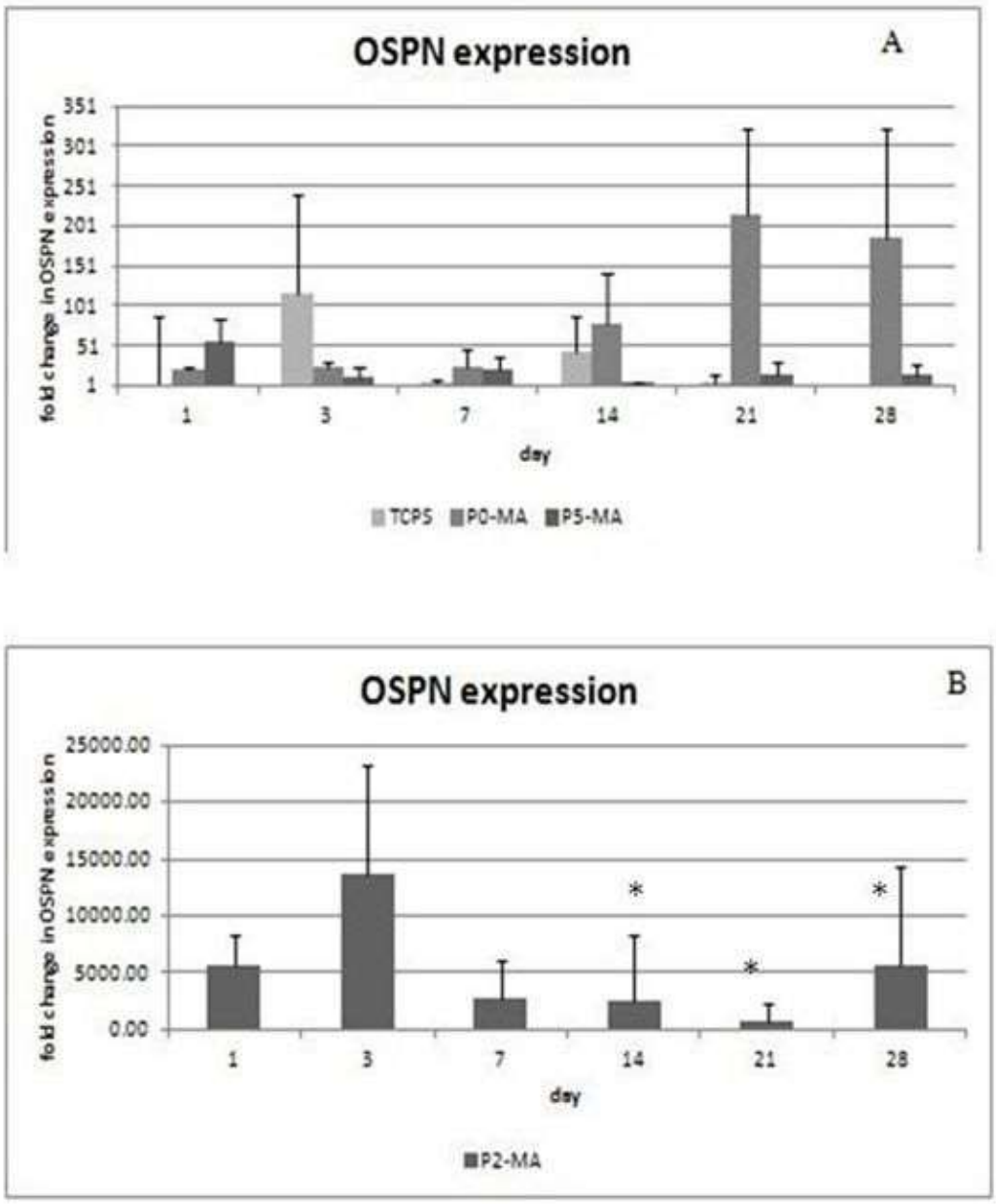

Figure 10. Messenger RNA expression levels of OSPN bone marker after 1, 3, 7, 14, 21 and 28 days of culture MC3T3-E1 cells on: (a) TCPS-control, P0-MA, P5-MA scaffolds, (b) P2-MA scaffold. Data have been normalized to the housekeeping gene GAPDH using TCPS as control sample. The results are shown as $2^{-\Delta\Delta CT}$. *$p < 0.05$ compared with the TCPS (control)

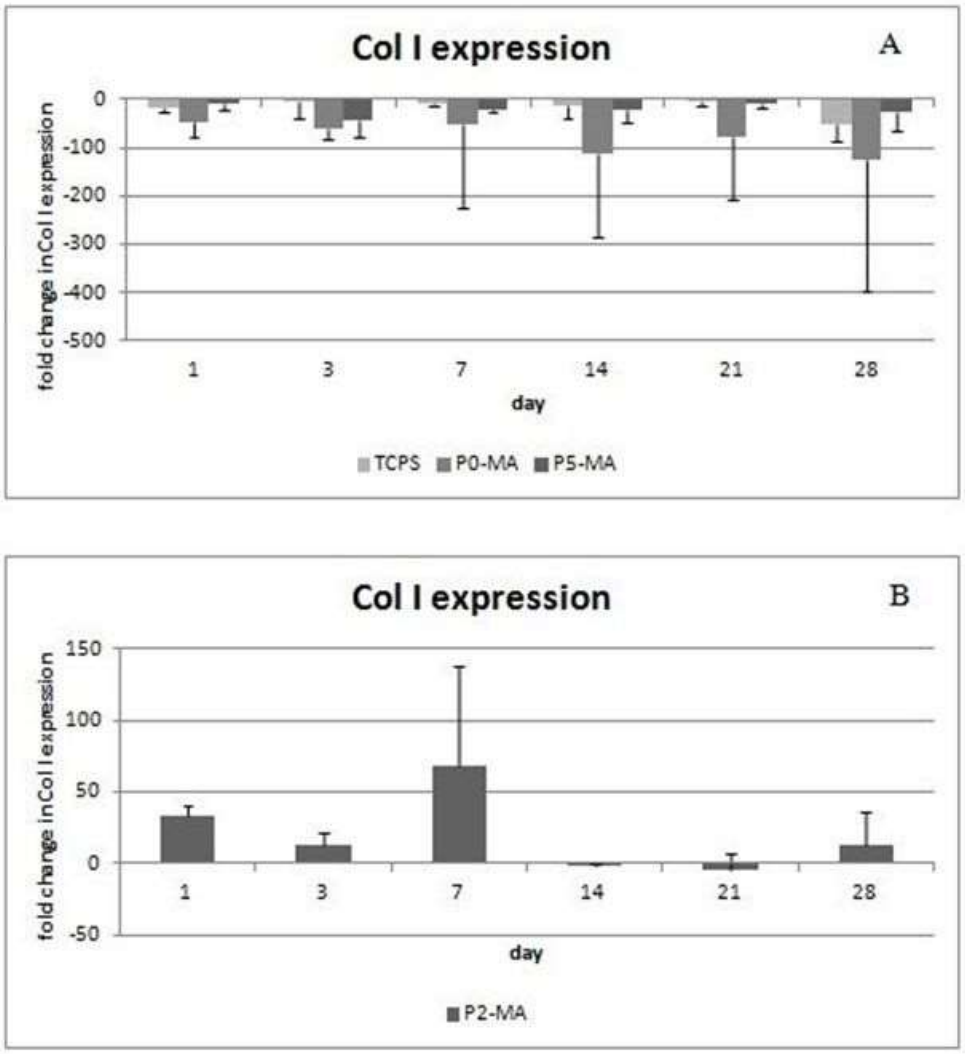

Figure 11. Messenger RNA expression levels of COL I bone marker after 1, 3, 7, 14, 21 and 28 days of culture MC3T3-E1 cells on (a) TCPS-control, P0-MA P5-MA scaffolds, (b) P2-MA scaffold. Data have been normalized to the housekeeping gene GAPDH using TCPS as control sample. The results are shown as $2^{-\Delta\Delta CT}$. *$p < 0.05$ compared with the TCPS (control)

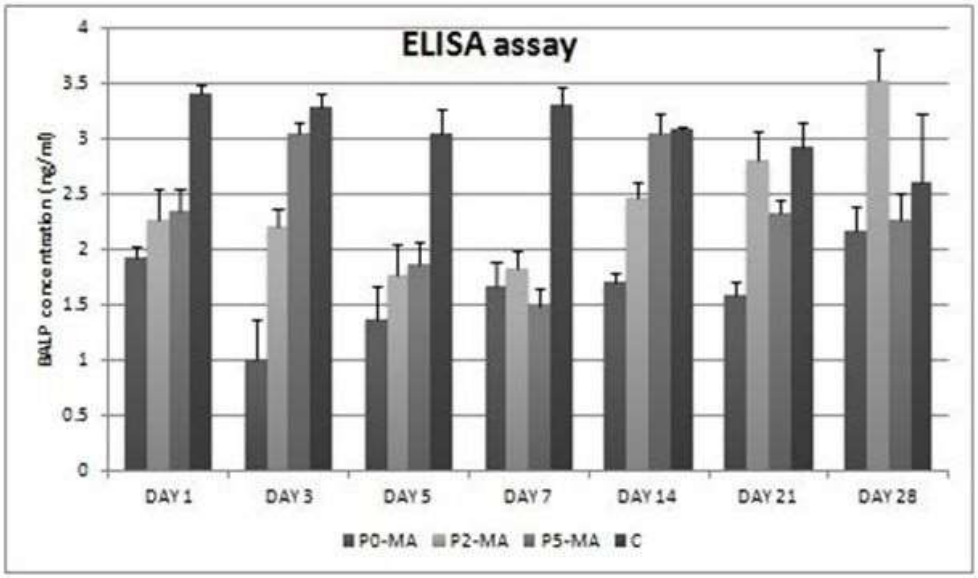

Figure 12. Bone alkaline phosphatase (ALP) activity of electrospun composite scaffolds seeded with MC3T3-E1 over 28 days. Enzyme activity was measured from the release from constructs into the cell culture medium. Experimental groups were P0-MA, P2-MA and P5-MA. Data represent means ± standard deviation for n=3.

Sample Code	% PHBV	%nHAp	%SF
P0	15	0	0
P2	15	2	2
P5	15	5	5

Table 1. Sample and treatment codes for electrospun samples and post-processed scaffolds